Check for updates

ADVANCED FUNCTIONAL MATERIALS
www.afm-journal.de

Sustainable and Circular Management of Perovskite Solar Cells via Green Recycling of Electron Transport Layer-Coated Transparent Conductive Oxide

*Valentina Larini, Changzeng Ding, Fabiola Faini, Giovanni Pica, Giovanna Bruni, Lorenzo Pancini, Silvia Cavalli, Matteo Manzi, Matteo Degani, Riccardo Pallotta, Michele De Bastiani, Chang-Qi Ma, and Giulia Grancini**

Transparent conductive oxide (TCO)-coated glasses are the most expensive and environmentally impacting components of perovskite solar cells (PSCs), comprising 56% of the total cost of a perovskite module and 96% of its carbon footprint. Thus, recycling TCO glasses from end-of-life perovskite modules can reduce both their levelized cost of electricity and energy payback time. In this work, tin oxide (SnO_2)-coated indium tin oxide glasses are refurbished from n-i-p PSCs employing dimethyl sulfoxide as a green solvent to dissolve the upper layers of the devices. Employing the recovered substrates, new-generation PSCs are produced, which retain the same champion power conversion efficiency (PCE) of 22.6% as fresh samples and display an even higher average PCE. This performance enhancement is investigated through compositional and electrical analyses that demonstrate that the proposed recycling protocol induces beneficial surface modifications on the SnO_2/perovskite interface and trap passivation, boosting charge extraction.

1. Introduction

Perovskite solar cells (PSCs) are an emerging photovoltaic (PV) technology that has witnessed exceptionally rapid progress for its extraordinary optical and electrical properties.[1] PSCs, which achieve at present 25.8% record power conversion efficiency (PCE), are also solution-processable technologies and can be fabricated using commercial, low-energy coating methods.[2,3] This represents a significant advantage to reduce the cost of the manufacturing process, making the levelized cost of electricity (LCOE) of PSCs competitive with the best crystalline silicon technologies.[4] As a consequence, PSCs stand out for their small energy payback time (EPBT) compared to mainstream technologies.[5] Nowadays, considerable efforts have been placed both from the academic and industrial sectors with the aim of advancing PSCs toward their commercialization.[6] In this regard, several device configurations and architectures have been proposed as scalable prototypes over the years. For instance, a technical report by the National Renewable Energy Laboratory (NREL) in 2021 provides an estimation of the manufacturing costs of a sheet-to-sheet n-i-p perovskite module.[7] The extrapolated materials costs are displayed as percentages in **Figure 1**a. The resulting pie chart shows that the transparent conductive oxide (TCO) glass, coated with the electron transport layer (ETL), largely outweighs all other constituents, clearly indicating its huge impact on manufacturing costs. In terms of sustainability, Tian et al.[6] recently performed a life cycle assessment (LCA) analysis on PSCs, revealing that the most environmentally impacting component of devices composed of indium tin oxide (ITO) glass, tin oxide (SnO_2), $N^2,N^2,N^{2\prime},N^{2\prime},N^7,N^7,N^{7\prime},N^{7\prime}$-octakis(4-methoxyphenyl)−9,9′-spirobi[9H-fluorene]−2,2′,7,7′-tetramine (spiro-OMeTAD), and copper is the ITO glass, as displayed by the pie chart of Figure 1b. Moreover, they estimated that by recycling key components of a PSC, its LCOE, EPBT, primary energy consumption, and greenhouse gas emission factor can be reduced by 0.16–0.59 cents kWh^{-1}, 52.6%, 50.9%, and 51.5%, respectively.[6]

V. Larini, F. Faini, G. Pica, L. Pancini, S. Cavalli, M. Manzi, M. Degani, R. Pallotta, M. De Bastiani, G. Grancini
Department of Chemistry & INSTM
University of Pavia
Via T. Taramelli 14, Pavia 27100, Italy
E-mail: giulia.grancini@unipv.it

C. Ding, C.-Q. Ma
Innovation Laboratory & Printable Electronics Research Center
Suzhou Institute of Nano-Tech and Nano-Bionics (SINANO)
Chinese Academy of Sciences (CAS)
Ruoshui Road 398, Suzhou 215123, China

G. Bruni
Department of Chemistry & CSGI
University of Pavia
via Taramelli 16, Pavia 27100, Italy

The ORCID identification number(s) for the author(s) of this article can be found under https://doi.org/10.1002/adfm.202306040

© 2023 The Authors. Advanced Functional Materials published by Wiley-VCH GmbH. This is an open access article under the terms of the Creative Commons Attribution-NonCommercial-NoDerivs License, which permits use and distribution in any medium, provided the original work is properly cited, the use is non-commercial and no modifications or adaptations are made.

DOI: 10.1002/adfm.202306040

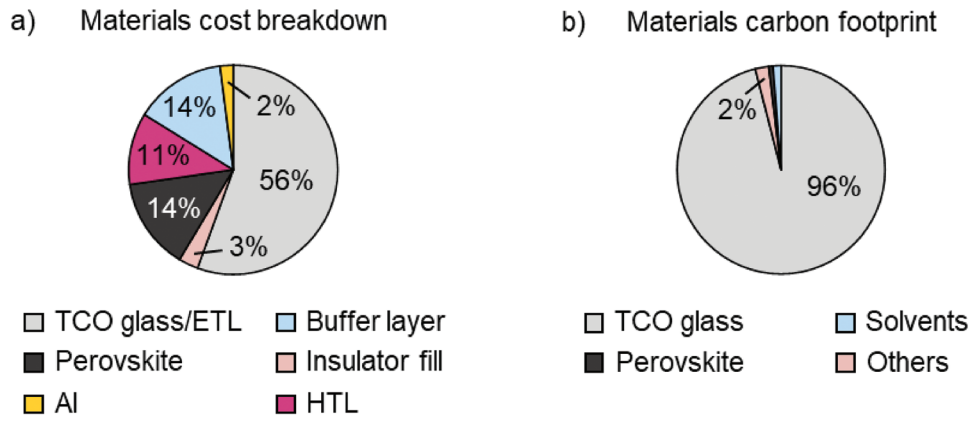

Figure 1. a) Pie chart reporting the materials cost breakdown of an n-i-p perovskite solar module (PSM). Data are extrapolated from.[7] b) Pie chart displaying the carbon footprint impact of constituting materials of an n-i-p PSM. Data are extrapolated from.[6]

Since TCO glass substrates are the costliest and most impacting components, several efforts have been devoted to recycling TCO glasses from end-of-life PSCs. However, the majority of previous works employ toxic dimethylformamide (DMF) to dissolve the upper layers of the solar cell. DMF is a hazardous solvent both for human health and the environment, included in the candidate list of substances of very high concern, as part of the regulation by the European Chemical Agency.[8] DMF can be absorbed into the human body through the respiratory system, skin, and digestive organs, causing prenatal toxicity and cancer.[9,10,11] Moreover, its end-of-life treatment impacts global warming and fine particulate matter formation.[8] Nevertheless, Ku et al.[12] employed DMF to restore a mesoporous nickel counter electrode from printable PSCs, Kadro et al.,[13] Huang et al.,[14] Zhu et al.[15] and Chowdhury et al.[16] used DMF on mesoporous titanium oxide (TiO_2)/fluorine-doped tin oxide (FTO)-based PSCs, while Huang et al.[17] adopted DMF to reuse ETL-free FTO substrates. In a relatively recent publication, a "one-key bleacher solution" was used to simultaneously and selectively dissolve all components of the PSC.[18] However, the "bleacher" solution was composed of methylamine and tetrahydrofuran, another highly toxic and hazardous solvent.[19,20] On the contrary, little evidence has been produced on the efficacy of less toxic and environmentally friendly (also called "green") solvents to recycle TCO substrates for PSCs, despite being pivotal. Augustine et al.[21] adopted a potassium hydroxide solution in deionized water to remove the upper layers of p-i-n PSCs thus recycling the ITO glass substrate. Nevertheless, the devices PCE, which was already quite low (8.15%) was further reduced by 12% upon recycling. More recently, Feng et al.[22] managed to recover nickel oxide/ITO substrates from p-i-n PSCs employing dialkylamines to dissolve the perovskite layer and the hole transport layer (HTL). Both works employed p-i-n PSCs configuration, but n-i-p is usually more commonly adopted in record-efficiency devices.[23] However, environmentally friendly and human health-safe recycling protocols have not been produced for the n-i-p configuration yet.

In this work, we develop a method to recycle SnO_2-coated ITO glass substrates of n-i-p PSCs employing the green solvent dimethyl sulfoxide (DMSO) to dissolve the upper layers of the device up to the metal oxide ETL. DMSO is a polar aprotic solvent that has a lower impact on the environment than DMF and is classified as a non-hazardous substance according to the Registration, Evaluation, Authorisation, and Restriction of Chemicals (REACH) registration (see Supporting Information). We demonstrate the validity of DMF replacement with DMSO in the development of a recycling protocol for PSCs. Indeed, by adopting our protocol, we fabricate recycled PSCs that retain 100% of the initial PCE, with even better average statistics, achieving a 22.6% PCE for the champion device. We investigate the reasons behind such an average performance improvement by analyzing the surface composition of fresh and recycled ETL/ITO glass substrates. We identify substantial changes in the energetics (electron properties) of the ETL surface, which we correlate to modifications in charge carrier recombination and charge extraction dynamics occurring at the ETL/perovskite interface. Such variations are then associated with the morphological and optical properties of fresh and recycled samples.

2. Results

Figure 2 displays a scheme of the recycling protocol designed for the recovery of ETL-coated ITO glass substrates. The recycling process consists in peeling off the metal electrode (gold in our case), followed by the simultaneous removal of HTL and perovskite layer employing a polar aprotic solvent. We employed either DMF or DMSO to demonstrate their equal ability to effectively remove the upper layers of the devices. Being the ETL a metal oxide, it remains firmly attached to the TCO when the substrates are dipped in the solvents. This allows for a smart recovery of the glass/TCO/ETL substrate to produce second-generation PSCs.

To demonstrate the efficacy of the recycling process, we produced n-i-p PSCs, whose architecture is schematically presented in **Figure 3**a, employing both fresh and recycled SnO_2/ITO glass substrates. Figure 3b shows the current density–voltage (*J*–*V*) characteristics in forward and reverse scan (FS and RS) of champion devices fabricated with fresh and recycled (with DMF or DMSO) SnO_2/ITO substrates, whose PV parameters are reported in **Table 1**. The three PSCs display similar PCE – 22.6%, 22.1%, and 22.6% for the fresh sample, the sample recycled with DMF, and the sample recycled with DMSO, respectively. These values resulted from the compensation between a slight decrease in

© 2023 The Authors. Advanced Functional Materials published by Wiley-VCH GmbH

16163028, 0, Downloaded from https://onlinelibrary.wiley.com/doi/10.1002/adfm.202306040 by Suzhou Institute Of Nano-Tech, Wiley Online Library on [15/01/2024]. See the Terms and Conditions (https://onlinelibrary.wiley.com/terms-and-conditions) on Wiley Online Library for rules of use; OA articles are governed by the applicable Creative Commons License

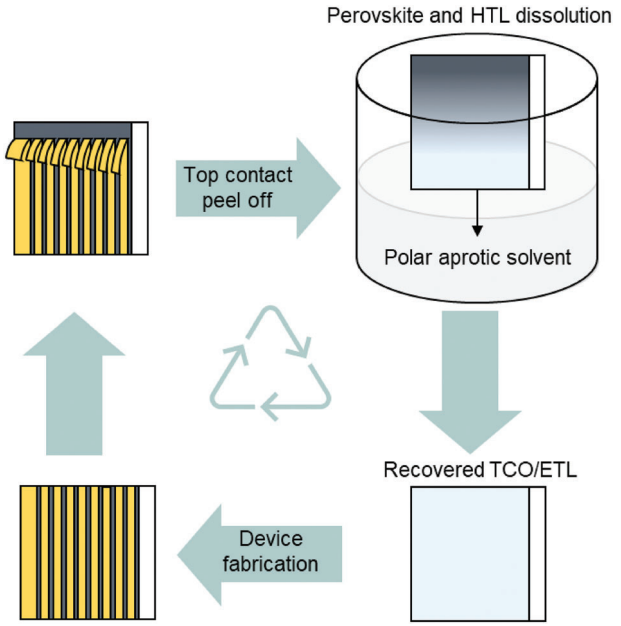

Figure 2. Scheme of the recycling protocol of transparent conductive oxide (TCO)/glass substrates. The metal electrode is peeled off, followed by the dissolution of the hole transport layer (HTL) and perovskite with a polar aprotic solvent. The electron transport layer (ETL) is recovered along with the TCO substrate, which is reused to fabricate a second-generation device.

open-circuit voltage (V_{OC}) and an increase in fill factor (FF) upon recycling. The statistical dispersion and mean value (represented as a horizontal line) for each PV parameter are displayed in the box charts of Figure 3c–f. While the mean V_{OC} decreases by 4% after recycling, the short-circuit current density (J_{SC}) slightly increases by 1%. However, the most relevant variation is displayed by the FF, which increases by 13% after recycling, ultimately leading to an overall 10% relative increment in the average PCE of the recycled PSCs. Incident photon-to-current efficiency (IPCE) curves are reported in Figure S1 (Supporting Information). While there is no change in the band gap of the three samples, the curves of DMF and DMSO recycled samples are shifted upwards, in line with a minimal reduction in the transmittance spectra (Figure S2, Supporting Information). Moreover, the mean hysteresis index of recycled devices is lower in absolute value with respect to fresh samples, as displayed in the box chart of Figure S3 (Supporting Information). Finally, Figure S4 (Supporting Information) presents the stability ratio ($\Delta_{stability}$ = performance of fresh sample at time X / performance of recycled samples at time X) between PSCs fabricated with fresh and recycled SnO_2/ITO glass substrates, which was evaluated by performing 1000 h of maximum power point tracking at 1 Sun illumination. Both Rec. DMF and Rec. DMSO devices show better stability than Fresh samples during the first 300 h of operation, while from 300 to 1000 h their behaviors equalize. For all PV parameters, there is no difference between devices fabricated with substrates recycled with DMF or DMSO. Since DMSO is a viable greener alternative to the more commonly employed DMF, due to its preferable LCA and environmental, health, and safety properties and its non-hazardous classification according to REACH registration (see Supporting Information), further comparisons will be performed between fresh and DMSO-recycled samples.[8]

Table 1. Photovoltaic parameters for forward and reverse scan (FS and RS) of champion devices fabricated with fresh and recycled, either with DMF or DMSO, SnO_2/ITO glass substrates.

Sample	V_{OC} [V]	J_{SC} [mAcm^{-2}]	FF [%]	PCE [%]
Fresh FS	1.14	24.7	79.5	22.4
Fresh RS	1.14	24.7	79.9	22.6
Recycled with DMF FS	1.09	25.1	82.0	22.5
Recycled with DMF RS	1.07	25.1	82.5	22.1
Recycled with DMSO FS	1.12	24.8	80.6	22.5
Recycled with DMSO RS	1.11	24.8	82.1	22.6

To clarify the origin of improvements behind the PV parameter trends, we performed X-ray photoelectron spectroscopy (XPS) on fresh and recycled SnO_2/ITO glass substrates and used formamidinium lead iodide ($FAPbI_3$), deposited onto ITO glass, as a control sample (**Figure 4**a). As shown by the magnification in Figure 4b, there are two peaks related to the presence of K on the surface of fresh SnO_2/ITO glass that disappear upon recycling. Similar results are provided by the time of flight – secondary ion mass spectroscopy (ToF-SIMS) K^+ surface maps of fresh and recycled SnO_2/ITO glass substrates, shown in Figure 4c. While fresh samples present a homogeneous distribution of K^+ throughout their surface, recycled substrates display no evidence of the cation. From a work published by Bu et al.,[24] we know that K^+ ions are included in the formulation of the SnO_2 Alfa Aesar precursor solution. Figure S5 (Supporting Information) reports scanning electron microscopy (SEM) images and SEM-Energy Dispersive X-ray (EDX) analysis of fresh and recycled SnO_2/ITO glass substrates, which demonstrate the presence of K-based crystallites on the surface of fresh samples that disappear after the recycling process. Further investigation is needed to determine the nature of such crystallites, which could consist either of a single substance or a compound or an oxidized or hydrolyzed form of K. From cross-section SEM images (Figure S6, Supporting Information), we could not identify any relevant difference in the structure of the perovskite growing on top of K-rich or K-free SnO_2 surface. The K-based crystallites removal upon recycling is further confirmed by atomic force microscopy images (AFM), presented in Figure S7 (Supporting Information), which reveal a reduction in the root mean square roughness (0.12 nm and 0.05 nm for fresh and recycled samples, respectively) of the SnO_2 surface after recycling.

Figure 4d is a magnification of the 125–155 eV range of Figure 4a, which highlights the Pb 4f XPS signals.[16] While the fresh sample does not display (as expected) any signal related to Pb, two peaks are present in the recycled substrate in correspondence with those shown by the $FAPbI_3$ control sample, suggesting the presence of residual Pb on the surface of recycled SnO_2/ITO glass substrates. ToF-SIMS Pb^{2+} surface maps of fresh and recycled SnO_2/ITO glass substrates (Figure 4e) corroborate these results, revealing the absence of Pb^{2+} on the surface of fresh samples and a uniform distribution of the cation on recycled substrates. We quantified the amount of Pb traces in the recycled sample using a fluorimetric Pb detection

© 2023 The Authors. Advanced Functional Materials published by Wiley-VCH GmbH

16163028, 0, Downloaded from https://onlinelibrary.wiley.com/doi/10.1002/adfm.202306040 by Suzhou Institute Of Nano-Tech, Wiley Online Library on [15/01/2024]. See the Terms and Conditions (https://onlinelibrary.wiley.com/terms-and-conditions) on Wiley Online Library for rules of use; OA articles are governed by the applicable Creative Commons License

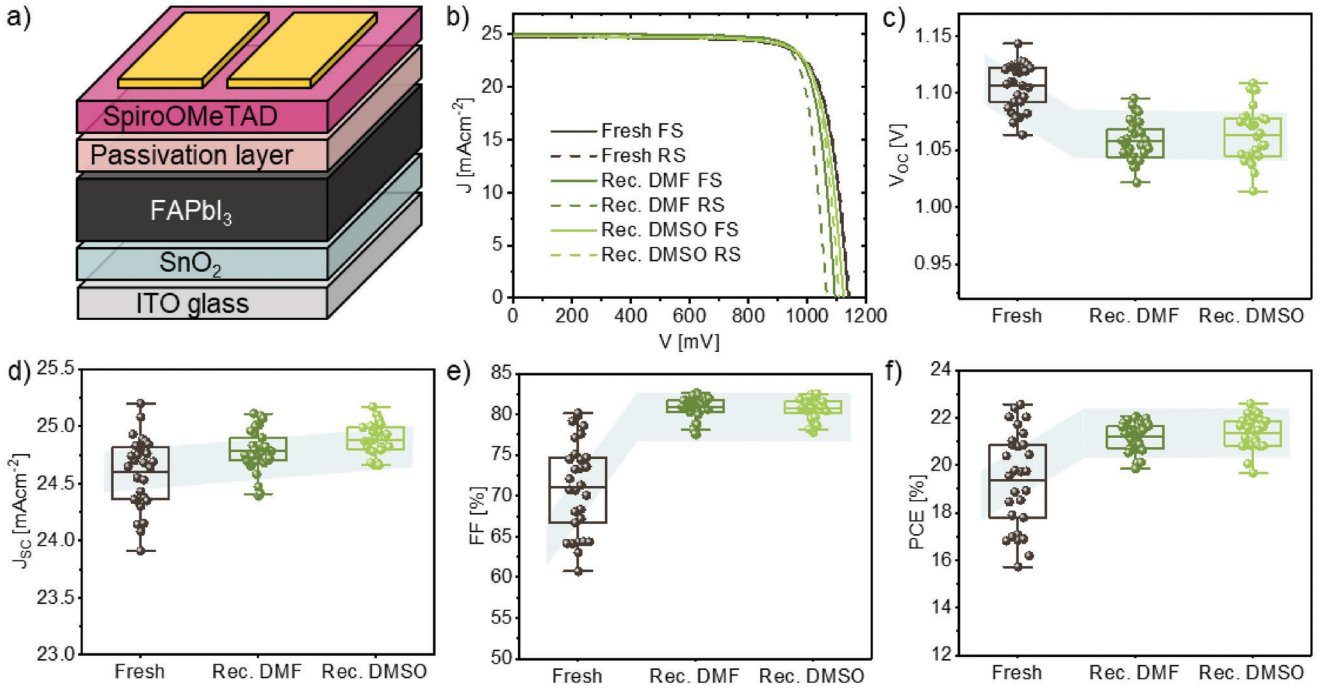

Figure 3. a) Schematic representation of the stack of the fabricated n-i-p perovskite solar cells (PSCs). b) Current density–voltage (*J–V*) curves in forward and reverse scan (FS, RS) of the best-performing devices fabricated employing fresh and recycled SnO_2/ indium tin oxide (ITO) glass. For recycling, dimethylformamide (DMF) and dimethyl sulfoxide (DMSO) solvents were compared and the related results are indicated as "Rec. DMF" and "Rec. DMSO", respectively. Box charts of c) V_{OC}, d) J_{SC}, e) FF, and f) PCE of PSCs fabricated with fresh, recycled with DMF and recycled with DMSO SnO_2/ITO glass substrates. Whiskers limit the 1.5 interquartile range, the box limits identify the 25th and 75th percentile and the horizontal line indicates the mean value. Sample size for Fresh, Rec. DMF and Rec. DMSO devices is 29, 40, and 30, respectively.

system (Figure S8, Supporting Information).[25] We determined a 0.3% Pb residual compared to a pristine $FAPbI_3$ film, which is equal to 1.5×10^{-3} mg cm^{-2}.

To understand the effects of the above-mentioned surface variations on the PV performances of PSCs, we performed the same washing steps of the recycling procedure onto fresh SnO_2/ITO glass substrates (before depositing the perovskite layer). Subsequently, we completed the fabrication of PSCs and analyzed their performances. The resulting box charts of the PV parameters are reported in **Figure 5**a and Figure S9 (Supporting Information), where samples subjected to the recycling washing steps are indicated as "Ref washed" and control samples are named "Ref". While the mean V_{OC} decreases upon washing the substrates, the average FF remains unchanged, overall leading to a lower PCE, further emphasized by a slight decrease in J_{SC}. These results suggest that the removal of K crystallites from the surface of fresh SnO_2/ITO glass substrates has a negative impact on the V_{OC} of the devices, but it does not affect their FF, which must be influenced by the perovskite removal and the consequent residual Pb traces remaining on the ETL surface.

Aiming at clarifying the causes of the V_{OC} reduction upon recycling, we performed time-resolved photoluminescence (TRPL) and photoluminescence quantum yield (PLQY) on devices fabricated with fresh and recycled SnO_2/ITO glass substrates. Figure 5b and Table S1 (Supporting Information) summarize the results. We collected TRPL traces on full devices before the evaporation of the metal contacts using a customized optical setup in which the excitation was provided by a 470 nm pulsed laser with a fluence of 0.2 uJ cm^{-2} corresponding to an excitation density of 4×10^{16} cm^{-3}.[26] In this regime, the PL decay can be fitted by a bi-exponential fit function $y = A_1 e^{\frac{-t}{\tau_1}} + A_2 e^{\frac{-t}{\tau_2}}$ where t_1 and t_2 are the decay constants and A_1 and A_2 the amplitudes of each decay component. The value of the shorter lifetime t_1 is unchanged between the statistical error for fresh and recycled samples ($t_1 = 3.0 \pm 0.8$ ns and $t_1 = 2.5 \pm 0.8$ ns, respectively), while t_2 decreases by 24% relative after the recycling protocol (from 83 ± 3 ns to 67 ± 7 ns), suggesting for worse quality of the perovskite in the recycled sample, being t_2 related to the bimolecular radiative recombination mechanisms occurring in the active material.[23] To further corroborate these hypotheses, we investigated the overall quality of the perovskites through PLQY analysis. We measured the PLQY of glass ITO/SnO_2/perovskites in the same experimental condition of TRPL analysis. The quenching of PLQY value of 29% after the recycling process (inset in Figure 5b) mirrors the behavior of t_2 extrapolated from TRPL analysis, indicating a favored non-radiative recombination mechanism, which explains the V_{OC} trend observed in the devices. To confirm these results, we conducted transient photovoltage (TPV) measurements on PSCs fabricated with fresh and recycled SnO_2/ITO glass substrates, which are reported in Figure 5c. Recycled samples display a faster decay, with a carrier lifetime of 2.1 µs, while fresh devices exhibit a decay time of 4.0 µs. A shorter carrier lifetime can induce higher charge recombination, resulting in a V_{OC} reduction, in agreement with PL analyses.[27] Thus, the removal of K-based

© 2023 The Authors. Advanced Functional Materials published by Wiley-VCH GmbH

16163028, 0, Downloaded from https://onlinelibrary.wiley.com/doi/10.1002/adfm.202306040 by Suzhou Institute Of Nano-Tech, Wiley Online Library on [15/01/2024]. See the Terms and Conditions (https://onlinelibrary.wiley.com/terms-and-conditions) on Wiley Online Library for rules of use; OA articles are governed by the applicable Creative Commons License

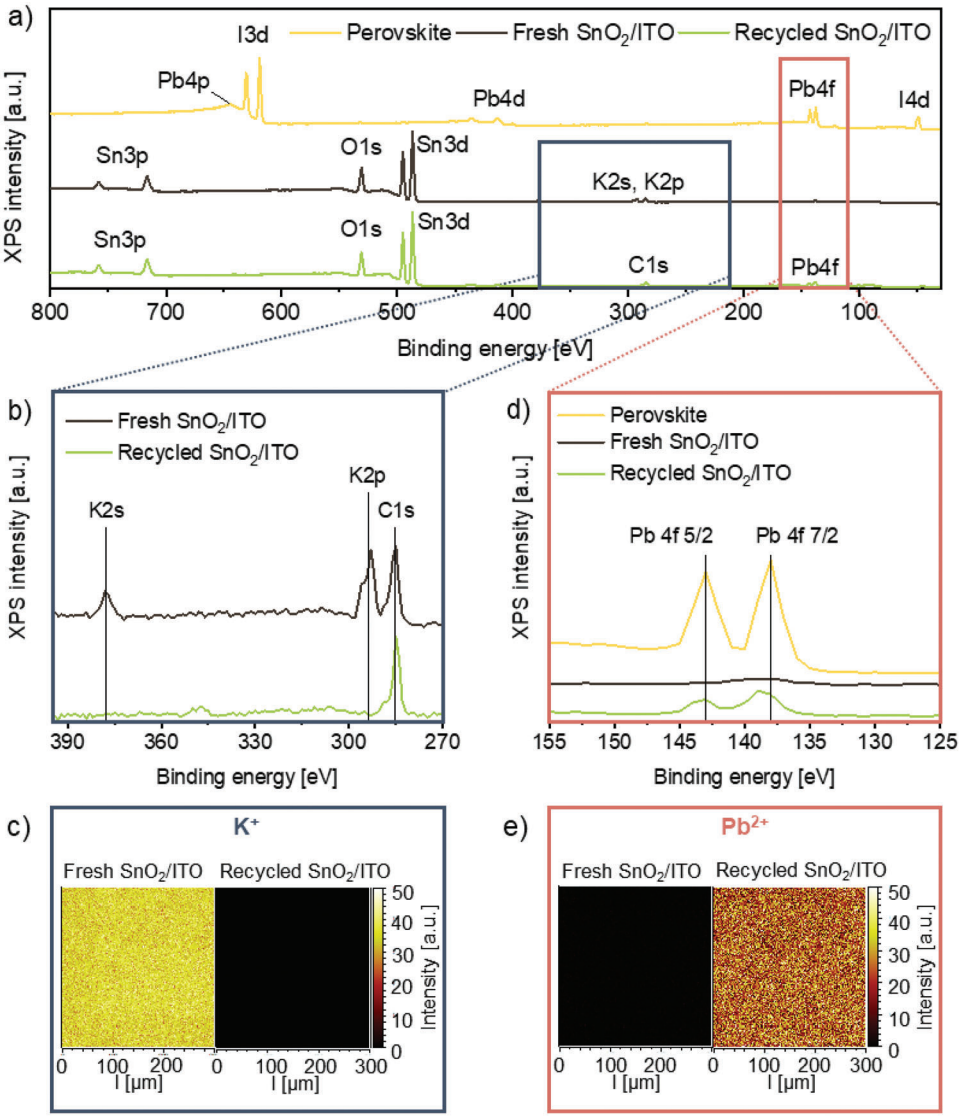

Figure 4. a) X-ray photoelectron spectroscopy (XPS) of $FAPbI_3$/ITO glass and fresh and recycled SnO_2/ITO glass substrates. Peak assignments are reported on the graph. b) Magnification of the 270–395 eV range, which highlights the potassium (K)-related peaks for fresh and recycled SnO_2/ITO glass. c) Magnification of the 125–155 eV range, which points out the lead (Pb)-related peaks for perovskite and fresh and recycled SnO_2/ITO glass. d) Time of flight – secondary ion mass spectroscopy (ToF-SIMS) K^+ surface maps of fresh and recycled SnO_2/ITO glass substrates. e) ToF-SIMS Pb^{2+} surface maps of fresh and recycled SnO_2/ITO glass substrates.

crystallites from the surface of SnO_2 upon recycling has a negative impact on the ETL/perovskite interface. Indeed, Bu et al.[24] report that K ions act as passivants on the surface of SnO_2, leading to an enhancement of the device performance. In our work, however, the mean V_{OC} reduction, induced by the recycling process adopted on PSCs, is fully compensated by an increase in the average FF.

In order to understand the reasons behind the FF improvement upon recycling, we performed transient photocurrent (TPC) analyses on devices fabricated with fresh and recycled substrates (Figure 5d). The TPC transients show a longer charge transport time for the fresh samples (2.3 μs) and a shorter time (1.2 μs) for the recycled devices. The faster photocurrent decay of recycled samples indicates a faster charge extraction, which can be related to the FF improvement.[28] We speculate that charge extraction enhancement is related to the presence of Pb residuals on the surface of recycled SnO_2/ITO glasses. Indeed, several works report that PbI_2 at the ETL/perovskite interface acts as holes sink thanks to its wide bandgap of 2.3 eV and prevents recombination between holes from the ETL and electrons from the perovskite layer, thus favoring charge extraction.[29,30,31] Furthermore, ultraviolet photoelectron spectroscopy (UPS) curves (Figure S10, Supporting Information) of fresh and recycled SnO_2/ITO glass substrates show a downward shift of the work function (WF) and the conduction band minimum (CBM) of SnO_2 upon recycling. While the WF reduction, from −3.1 to

© 2023 The Authors. Advanced Functional Materials published by Wiley-VCH GmbH

16163028, 0, Downloaded from https://onlinelibrary.wiley.com/doi/10.1002/adfm.202306040 by Suzhou Institute Of Nano-Tech, Wiley Online Library on [15/01/2024]. See the Terms and Conditions (https://onlinelibrary.wiley.com/terms-and-conditions) on Wiley Online Library for rules of use; OA articles are governed by the applicable Creative Commons License

16163028, 0, Downloaded from https://onlinelibrary.wiley.com/doi/10.1002/adfm.202306040 by Suzhou Institute Of Nano-Tech, Wiley Online Library on [15/01/2024]. See the Terms and Conditions (https://onlinelibrary.wiley.com/terms-and-conditions) on Wiley Online Library for rules of use; OA articles are governed by the applicable Creative Commons License

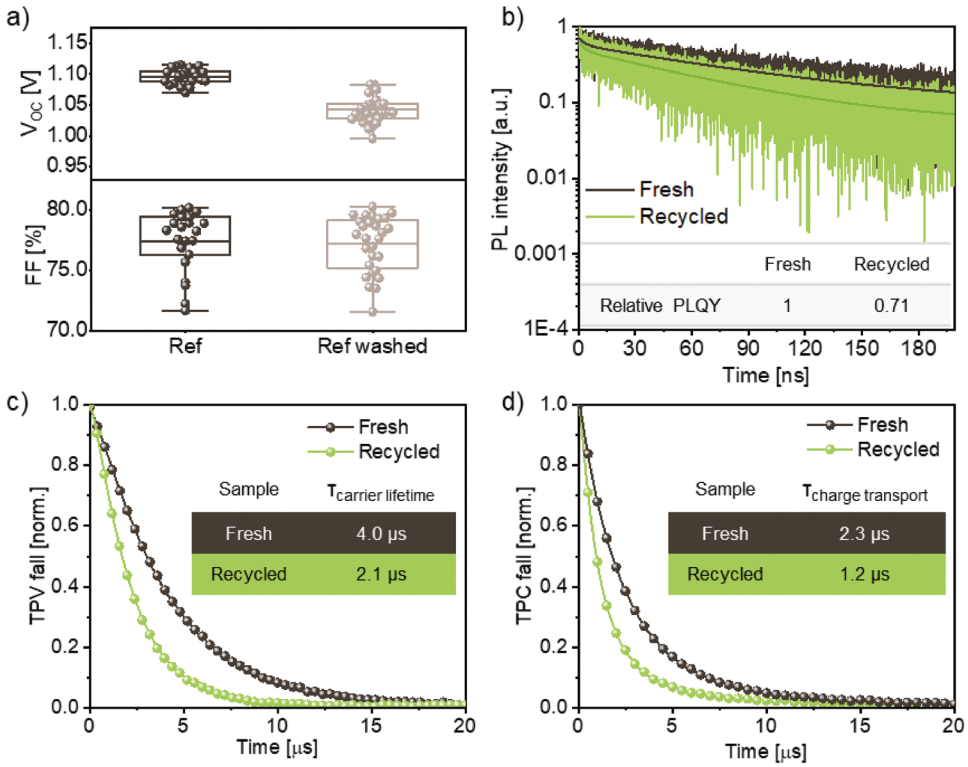

Figure 5. a) V_{OC} and FF box charts of PSCs fabricated with fresh SnO_2/ITO glass substrates with or without further washing steps after SnO_2 deposition. Whiskers limit the 1.5 interquartile range, the box limits identify the 25th and 75th percentile and the horizontal line indicates the mean value. Sample size for Ref and Ref washed devices is 22 and 28, respectively. b) Time-resolved photoluminescence (TRPL) of spiro-OMeTAD/passivation layer/perovskite/SnO_2/ITO glass devices fabricated with fresh and recycled SnO_2/ITO glass substrates. The inset reports their relative photoluminescence quantum yield (PLQY). c) Transient photovoltage (TPV) and d) transient photocurrent (TPC) decays of PSCs fabricated with fresh and recycled SnO_2/ITO glass substrates. Decay times are reported in the insets.

−3.7 eV, is in accordance with the V_{OC} reduction, the downshifted CBM suggests an improved charge extraction, therefore confirming TPC results.

3. Conclusion

In summary, we demonstrated a green recycling protocol to recover SnO_2-coated ITO glass substrates from n-i-p PSCs employing DMSO as a solvent to dissolve the upper layer of the device. The obtained recycled substrates were used to fabricate second-generation PSCs, which displayed the same champion PCE as fresh PSCs. Furthermore, a slight decrease in the mean V_{OC} was extensively compensated by a FF increase, which lead to an overall average PCE enhancement. On one hand, the V_{OC} reduction upon recycling was attributed to higher non-radiative recombination, which was a consequence of the removal of K from the surface of recycled SnO_2/ITO glass substrates. On the other hand, the FF improvement was associated with a faster and more efficient charge extraction, promoted by the presence of a residual amount of Pb (in the order of 10^{-3} mg cm^{-2}) on the surface of recycled SnO_2/ITO. Overall, our work contributes to advance in the rational design of recycling methods to improve PSCs sustainability. Due to the wide versatility of the developed process, we believe that our recycling method can be effectively applied to other ETL systems, such as TiO_2-based PSCs, as well as to PSCs in p-i-n configuration. By recovering TCO glass substrates from end-of-life perovskite PVs, their economic and environmental impact will be reduced, easing the potential entry of PSCs into the PV market.

4. Experimental Section

Materials: Chlorobenzene (CB, extra dry, 99.8%), dimethyl sulfoxide (DMSO, ≥99.9% Extra Dry), and N,N-dimethylformamide (DMF, 99.8%, Extra Dry) were purchased from Acros Organics. Tin (iv) oxide (SnO_2 15% in H_2O) was purchased from Alfa Aesar. DMSO (Reagent Plus, ≥99.5%), acetone (≥99.8%), 2-propanol (IPA, ≥99.8%), N^2,N^2,N$^{2'}$,N$^{2'}$,N^7,N^7,N$^{7'}$,N$^{7'}$-octakis(4-methoxyphenyl)−9,9′-spirobi[9H-fluorene]−2,2′,7,7′-tetramine (Spiro-OMeTAD, 99%, HPLC), Bis(trifluoromethane)sulfonimide lithium salt (Li-salt, 99.95%), acetonitrile (ACN, anhydrous, 99.8%), and 4-tert-butylpyridine (4-tBP,98%) were purchased from Sigma-Aldrich. Lead iodide (PbI_2, >98.0%) was purchased from TCI. Formamidinium iodide (FAI, >99.99%), methylammonium chloride (MACl) and 4-methylphenethylammonium chloride (MePEACl) were purchased from GreatCell Solar Materials. Hellmanex III cleaning concentrate was purchased from Hellma.

Device Fabrication: For the fabrication of perovskite solar cells (PSCs), indium tin oxide (ITO)-coated glass substrates were consecutively cleaned in acetone and IPA by ultrasonicating for 15 min for each solvent. Substrates were dried with N_2 airflow and UV-ozone treated for 30 min. SnO_2 colloidal dispersion (10% in water) was spin-coated onto ITO/glass substrates and annealed at 150 °C for 30 min. Subsequently, SnO_2-coated substrates were subjected to UV-ozone treatment for 30 min. All

© 2023 The Authors. Advanced Functional Materials published by Wiley-VCH GmbH

solutions were prepared in an Ar-filled glovebox, while the deposition of each layer of the solar cell was performed in an N_2-filled glovebox. The perovskite precursor solution (1.2 M) was prepared by dissolving PbI_2, FAI, and MACl (35 mol%) in DMF/DMSO 4/1, with 5 mol% PbI_2 excess. The solution (25 µL) was deposited on the SnO_2-coated substrates and spin-coated with a three-step procedure: in the first step substrates were spun at 1000 rpm for 12 s, the second step proceeded at 5000 rpm for 27 s, while the last step was a speed reduction of 4 s. Ten seconds after the beginning of the second step, CB (150 µL) was dropped onto the spinning substrate for an antisolvent procedure. Subsequently, substrates were annealed at 150 °C for 30 min. For the passivation layer, 50 µL of a solution of MePEACl (0.01 M) in IPA was spin-coated onto the perovskite layer at 4000 rpm for 30 s and substrates were annealed at 100 °C for 10 min. To fabricate the HTL, Spiro-OMeTAD was dissolved in CB (80 mg mL^{-1}). The solution was doped by adding Li salt (17.5 µL) dissolved in ACN (500 mg mL^{-1} in ACN) and 4-tBP (28.8 µL) to 1 mL of Spiro-OMeTAD solution in CB. The solution (10 µL) was spin-coated onto the perovskite layer. Finally, 80 nm of Au was thermally evaporated on the device with a shadow mask of 0.0825 cm^2 area, producing devices of 0.045 cm^2 active area due to the overlap between evaporated gold and ITO. The evaporation speed was adjusted to 0.01 nm s^{-1} for the first 5 nm, 0.02 nm s^{-1} from 5 to 15 nm, and 0.06 nm s^{-1} for the rest of the procedure.

Device Recycling: To recycle SnO_2-coated ITO glass substrates from n-i-p PSCs, the Au top electrode was peeled off using scotch tape. Then, the perovskite layer and HTL were dissolved into either DMF or DMSO and the recovered ITO/SnO_2 substrates were consecutively cleaned in DMF or DMSO, Hellmanex III cleaning concentrate diluted in water, water, acetone, and IPA by ultrasonicating for 15 min for each solvent. Finally, substrates were dried with N_2 airflow, UV-ozone treated for 30 min, and employed for the fabrication of second-generation PSCs.

Characterization: Current density–voltage (*J–V*) characteristics of the produced PSCs were carried out using a Keithley 2400 sourcemeter and an Abet solar simulator. The simulated 1Sun AM1.5G illumination was calibrated using a certified Si reference cell (Open RR-1002, KG5 window). The devices were measured both in reverse scan (1.2 V →□ 0 V, 130 mVs^{-1}) and forward scan (0 →□ 1.2 V, 130 mVs^{-1}). During every measurement, a metal shadow mask with an aperture area of 0.03 cm^2 was used to cover the device's active area.

Incident-photon-to-current efficiency (IPCE) measurements were performed with a Cicci Research Arkeo steady-state tests module. The wavelength scan range was set between 300 and 900 nm with a scan step of 10 nm.

Transmittance curves were analyzed by UV-visible spectrometer (Lambda 750, PerkinElmer).

X-ray and ultraviolet photoelectron spectroscopy (XPS and UPS) analyses were conducted at a PHI 5000 VersaprobeII system.

Stability measurements were conducted by coupling a Wavelabs SINUS-70 solar simulator with a Fluxim Lithos Lite module and performing maximum power point tracking for 1000 h under an N_2 atmosphere at 1 sun illumination, employing a shadow mask of 1.25 mm^2 active area.

Time of flight – secondary ion mass spectroscopy (ToF-SIMS) surface maps were acquired with TOF.SIMS 5–100, with the pulsed primary ions from a Cs^+ (2 keV) ion gun for sputtering and a Bi^+ ion beam for analysis.

Scanning electron microscopy and energy dispersive X-ray spectroscopy analyses were carried out by a Zeiss EVO MA10 (Carl Zeiss, Oberkochen, Germany) coupled with an EDS detector (X-max 50 mm^2, Oxford Instruments, Oxford, UK). Cross-section SEM images of PSCs were recorded with a SEM (Regulus8230) under 10 kV electron beam accelerate voltage.

Atomic force microscopy (AFM) measurements were performed with a TriA-SPM microscope (A.P.E. Research S.r.l., Trieste, Italy) in contact mode, using CSC17/AlBS probes (Mikromasch – Innovative Solutions Bulgaria Ltd.) applying a force of 60 nN and scanning an area of 5 × 5 µm. AFM images were edited with Gwyddion and root mean square roughness was calculated with an internal software function.

Time-resolved photoluminescence (TRPL) curves were collected using a customized optical setup in which the excitation was provided by pulsed/CW laser at 470 nm (PicoQuant) with a spot area of ≈70 $µm^2$. The luminescence was analyzed with an interferometer (GEMINI by Nireos) and recorded with a single photon detector (IDQuantique) coupled with a Time Tagger (Swabian Instrument). The scan was performed in pulsed mode (repetition rate of 5 MHz) using an energy fluence of 0.2 µJ cm^{-2}.

Photoluminescence quantum yield (PLQY) was carried out with a variation of the customized aforementioned optical setup in which the excitation was provided by the same laser at 470 nm and a repetition rate of 80 MHz allowing an energy fluence of 0.2 µJ cm^{-2}.

Transient photovoltage (TPV) and transient photocurrent (TPC) analyses were performed with a Cicci Research Arkeo transient tests module. Measurements were conducted under 1 Sun illumination and constant bias was perturbed with short light pulses of 200 µs width.

Statistical Analysis: For photovoltaic parameters statistical analysis, data were pre-processed by defining as outliers all values lying above or below the 1.5 interquartile range. The resulting dataset was arranged in box charts, where the upper and lower limits of the box identify the 25th and 75th percentile, respectively, while whiskers indicate the 1.5 interquartile range. The mean value for each sample is presented as a horizontal line within the box. Sample size (*n*) for Fresh, Rec. DMF and Rec. DMSO devices was 29, 40, and 30, respectively. OriginPro 2018 was employed for statistical analysis.

Supporting Information

Supporting Information is available from the Wiley Online Library or from the author.

Acknowledgements

The authors acknowledge Edison for the collaboration, the project for infrastructures funded by Regione Lombardia RL3776, the Fondazione Cariplo Economia Circolare 2021 Project ″Green flexible hybrid perovskite solar module for the market: from smart lead manipulation to recycling″ (FLHYPER, no 20201067), funded under the "Circular Economy-2020" call, the "HY-NANO" project that received funding from the European Research Council (ERC) Starting Grant 2018 under the European Union's Horizon 2020 research and innovation program (Grant Agreement No. 802862), the Ministero dell'Università e della Ricerca (MUR) and the University of Pavia through the program ″Dipartimenti di Eccellenza 2023–2027″. C.D. and C.-Q.M. acknowledge the technical support for Nano-X from Suzhou Institute of Nano-Tech and Nano-Bionics, Chinese Academy of Sciences (No. A2107).

Conflict of Interest

The authors declare no conflict of interest.

Data Availability Statement

The data that support the findings of this study are available from the corresponding author upon reasonable request.

Keywords

circular economy, perovskites, perovskite solar cells, recycling

Received: May 30, 2023
Revised: July 13, 2023
Published online:

© 2023 The Authors. Advanced Functional Materials published by Wiley-VCH GmbH

16163028, 0, Downloaded from https://onlinelibrary.wiley.com/doi/10.1002/adfm.202306040 by Suzhou Institute Of Nano-Tech, Wiley Online Library on [15/01/2024]. See the Terms and Conditions (https://onlinelibrary.wiley.com/terms-and-conditions) on Wiley Online Library for rules of use; OA articles are governed by the applicable Creative Commons License

[1] J. Y. Kim, J. W. Lee, H. S. Jung, H. Shin, N. G. Park, *Chem. Rev.* **2020**, *120*, 7867.
[2] NREL, Best Research-Cell Efficiency Chart, https://www.nrel.gov/pv/cell-efficiency.html (accessed: May 2023).
[3] A. S. R. Bati, Y. L. Zhong, P. L. Burn, M. K. Nazeeruddin, P. E. Shaw, M. Batmunkh, *Commun. Mater.* **2023**, *4*, 2.
[4] M. De Bastiani, V. Larini, R. Montecucco, G. Grancini, *Energy Environ. Sci.* **2022**, *16*, 421.
[5] J. Gong, S. B. Darling, F. You, *Energy Environ. Sci.* **2015**, *8*, 1953.
[6] X. Tian, S. D. Stranks, F. You, *Nat. Sustain.* **2021**, *4*, 821.
[7] B. L. Smith, M. Woodhouse, K. A. W. Horowitz, T. J. Silverman, J. Zuboy, R. M. Margolis, Technical Report NREL, https://www.nrel.gov/docs/fy22osti/78173.pdf. (accessed: May 2023).
[8] R. Vidal, J.-A. Alberola-Borràs, S. N. Habisreutinger, J.-L. Gimeno-Molina, D. T. Moore, T. H. Schloemer, I. Mora-Seró, J. J. Berry, J. M. Luther, *Nat. Sustain.* **2021**, *4*, 277.
[9] J. Lee, M. Hahm, D. A. Huh, S. H. Byeon, *Int J Environ Res Public Health* **2018**, *15*, 503.
[10] J. Hellwig, J. Merkle, H. Klimisch, R. Jackh, *Food Chem. Toxicol.* **1991**, *29*, 193.
[11] S. M. Levin, D. B. Baker, P. J. Landrigan, S. V. Monaghan, E. Frumin, M. Braithwaite, W. Towne, *Lancet* **1987**, *330*, 1153.
[12] J. M. Kadro, N. Pellet, F. Giordano, A. Ulianov, O. Müntener, J. Maier, M. Grätzel, A. Hagfeldt, *Energy Environ. Sci.* **2016**, *9*, 3172.
[13] L. Huang, Z. Hu, J. Xu, X. Sun, Y. Du, J. Ni, H. Cai, J. Li, J. Zhang, *Sol. Energy Mater. Sol. Cells* **2016**, *152*, 118.
[14] W. Zhu, W. Chai, D. Chen, H. Xi, D. Chen, J. Chang, J. Zhang, C. Zhang, Y. Hao, *ACS Appl. Mater. Interfaces* **2020**, *12*, 4549.
[15] M. S. Chowdhury, K. S. Rahmanb, V. Selvanathanb, A. K. M. Hasanb, M. S. Jamalbc, N. A. Samsudind, M.d. Akhtaruzzaman, N. Amin, K. Techato, *RSC Adv.* **2021**, *11*, 14534.
[16] L. Huang, J. Xu, X. Sun, R. Xu, Y. Du, J. Ni, H. Cai, J. Li, Z. Hu, J. Zhang, *ACS Sustainable Chem. Eng.* **2017**, *5*, 3261.
[17] Z. Ku, X. Xia, H. Shen, N. H. Tiep, H. J. Fan, *Nanoscale* **2015**, *7*, 13363.
[18] K. Wang, T. Ye, X. Huang, Y. Hou, J. Yoon, D. Yang, X. Hu, X. Jiang, C. Wu, G. Zhou, S. Priya, *Matter* **2021**, *4*, 2522.
[19] P. Shah, S. Parikh, M. Shah, S. Dharaskar, *Biomass Convers. Biorefinery* **2022**, *12*, 1985.
[20] D. R. Joshi, N. Adhikari, *J Pharm Res Int* **2019**, *3*, 1.
[21] B. Augustine, K. Remes, G. S. Lorite, J. Varghese, T. Fabritius, *Sol. Energy Mater. Sol. Cells* **2019**, *194*, 74.
[22] X. Feng, S. Wang, Q. Guo, Y. Zhu, J. Xiu, L. Huang, Z. Tang, Z. He, *J. Phys. Chem. Lett.* **2021**, *12*, 4735.
[23] S. Lan, W. Zheng, S. Yoon, H. U. Hwang, J. W. Kim, D.-W. Kang, J.-W. Lee, H.-K. Kim, *ACS Appl. Energy Mater.* **2022**, *5*, 14901.
[24] T. Bu, J. Li, F. Zheng, W. Chen, X. Wen, Z. Ku, Y. Peng, J. Zhong, Y.-B. Cheng, F. Huang, *Nat. Commun.* **2018**, *9*, 4609.
[25] L. Pancini, R. Montecucco, V. Larini, A. Benassi, D. Mirani, G. Pica, M. De Bastiani, F. Doria, G. Grancini, *Mater. Adv.* **2023**, *4*, 2410.
[26] G. Pica, D. Bajoni, G. Grancini, *Struct. Dyn.* **2022**, *9*, 011101.
[27] X. Huang, Q. Cui, W. Bi, L. Li, P. Jia, Y. Hou, Y. Hu, Z. Lou, F. Teng, *RSC Adv.* **2019**, *9*, 7984.
[28] S. Mabrouk, A. Dubey, W. Zhang, N. Adhikari, B. Bahrami, M. N. Hasan, S. Yang, Q. Qiao, *J. Phys. Chem. C* **2016**, *120*, 24577.
[29] Q. Chen, H. Zhou, T.-B. Song, S. Luo, Z. Hong, H.-S. Duan, L. Dou, Y. Liu, Y. Yang, *Nano Lett.* **2014**, *14*, 4158.
[30] M. C. Shih, S.-S. Li, C.-H. Hsieh, Y.-C. Wang, H.-D. Yang, Y.-P. Chiu, C.-S. Chang, C.-W. Chen, *Nano Lett.* **2017**, *17*, 1154.
[31] Z. Ahmad, R. A. Scheidt, M. P. Hautzinger, K. Zhu, M. C. Beard, G. Galli, *ACS Energy Lett.* **2022**, *7*, 1912.

© 2023 The Authors. Advanced Functional Materials published by Wiley-VCH GmbH

16163028, 0, Downloaded from https://onlinelibrary.wiley.com/doi/10.1002/adfm.202306040 by Suzhou Institute Of Nano-Tech, Wiley Online Library on [15/01/2024]. See the Terms and Conditions (https://onlinelibrary.wiley.com/terms-and-conditions) on Wiley Online Library for rules of use; OA articles are governed by the applicable Creative Commons License